CANADIAN APPLIED
MATHEMATICS QUARTERLY
Volume 1, Number 1, Winter 1993

MULTISTABILITY AND BOUNDARY LAYER DEVELOPMENT IN A TRANSPORT EQUATION WITH DELAYED ARGUMENTS

ALEJANDRO D. REY AND MICHAEL C. MACKEY

ABSTRACT. Here we consider cell population dynamics in which there is simultaneous proliferation and maturation. The mathematical model for this process is derived, and results in a nonlinear first order partial differential equation for the cell density $u(t,x)$ in which there is retardation in both temporal (t) and maturation (x) variables. Numerical analysis of a representative equation indicates that there are two classes of solution behavior depending on the initial function $\varphi(x)$. If $\varphi(0) > 0$ there is a unique stationary solution. In this case the net effect of the time delay is to retard the dynamic approach to the stationary solution, while spatial delays modify the steady state distributions with respect to the maturation variable. Alternately, if $\varphi(0) = 0$, the stationary solutions display a multistability that depends on the maturation velocity r. For a critical value $r = r_c$, which depends on the time delay, the stationary solution is nonhomogeneous. For values of r close to r_c, the solution dynamics exhibit critical slowing down, similar to that seen in the neighborhood of a phase transition. For $0 < r_c < r$, the stationary solution is uniformly zero, while for $0 < r < r_c$, the stationary solution is homogeneous and singular.

1. Introduction. A variety of mathematical models for biological dynamics are most appropriately framed as differential delay equations [11]. Many of these problems involve descriptions of cell replication, and in this circumstance the natural delay is the cell cycle time.

The purpose of this paper is twofold. We first show that, in a simple model in which cells are both proliferating and maturing, one obtains a dynamical equation that is a first order partial differential equation in which there is a retardation in the time variable as well as in a maturation variable. Second, because of the apparently novel nature of this problem and the paucity of relevant mathematical results, we numerically study the solution behavior of a prototypical system in which

Received by the editor on May 1, 1991, and in revised form on December 18, 1991.

the analytic solution in the absence of delays is easily constructed. We then individually examine the effect of the retardation effects on the time and maturation variables and then the full numerical behavior of the system.

2. A model for proliferating and maturing cellular populations. We consider a population of cells that is capable of both proliferation and maturation. Actively proliferating cells are those actually in cycle that are committed to the replication of their DNA and the ultimate passage through mitosis and cytokinesis with the eventual production of two daughter cells. The position of one of these cells within the cell cycle is denoted by a (cell *age*), which is assumed to range from $a = 0$ (the point of commitment) to $a = \bar{\tau}$ (the point of cytokinesis). In the most general situation in a population of cells, the age $\bar{\tau}$ at cytokinesis is not identical between cells, but is distributed with a density $f(\bar{\tau})$ supported on $[\tau_{\min}, \tau_{\max}]$ so $0 < \tau_{\min} \leq \bar{\tau} \leq \tau_{\max} < \infty$. In addition, each cell can be characterized by a maturation variable x whose range can be taken, without loss of generality, from $x = 0$ to $x = 1$. For concreteness, one could think of erythroid precursor cells and associate the maturation variable with the intracellular hemoglobin content. We assume that cells die at a rate $\gamma \geq 0$ independent of age or maturation level, and mature with a velocity $V(x)$. For more details concerning the biology of the cell cycle, consult [**2**].

If we denote the density of proliferating cells by $U(t, x, a)$, then the conservation equation for $U(t, x, a)$ is easily shown to be given by

$$\frac{\partial U}{\partial t} + \frac{\partial U}{\partial a} + \frac{\partial [V(x)U]}{\partial x} = -\gamma U, \tag{1}$$

with the initial condition

$$U(0, x, a) = \Gamma(x, a) \quad \text{for } (x, a) \in [0, 1] \times [0, \tau_{\max}]. \tag{2}$$

The total number u of proliferating cells of a given maturation level is defined in a natural way as

$$u(t, x) = \int_0^{\tau_{\max}} U(t, x, a)\, da. \tag{3}$$

In completing the formulation of this problem we specify a nonlinear boundary condition that captures the essence of the biology through

$$U(t,x,0) = 2\int_{\tau_{\min}}^{\tau_{\max}} f(\bar{\tau})U(t,x,\bar{\tau})\,d\bar{\tau} = \mathcal{F}(u(t,x)). \tag{4}$$

The first part of this boundary condition reflects the fact that the age at cytokinesis is distributed with density $f(\bar{\tau})$ and that the two daughter cells produced at the end of the cell division cycle form the input flux into the cell cycle. The second portion states that the input flux is a function $\mathcal{F}$ of the total number of cells at a given maturation level.

To proceed beyond this point, for concreteness we assume that the maturation velocity V has the form

$$V(x) = rx, \qquad r > 0, \tag{5}$$

though this is by no means necessary. Thus equation (1) becomes

$$\frac{\partial U}{\partial t} + \frac{\partial U}{\partial a} + rx\frac{\partial U}{\partial x} = -[\gamma + r]U, \tag{6}$$

with the same initial and boundary conditions stated before. The general solution of equation (6) is

$$U(t,x,a) = \begin{cases} \Gamma(xe^{-rt}, a-t)e^{-(\gamma+r)t} & 0 \le t \le a \\ U(t-a, xe^{-ra}, 0)e^{(\gamma+r)a} & a < t. \end{cases} \tag{7}$$

Integrating equation (6) over the age variable a gives

$$\frac{\partial u}{\partial t} + rx\frac{\partial u}{\partial x} = -[\gamma + r]u - \{U(t,x,\tau_{\max}) - U(t,x,0)\}. \tag{8}$$

Utilizing the general solution (7) in conjunction with the boundary condition (4) gives

$$\frac{\partial u}{\partial t} + rx\frac{\partial u}{\partial x} = -[\gamma + r]u + \psi \tag{9a}$$

where

$$\psi = \begin{cases} [2\int_0^{\tau_{\max}} f(\bar{\tau})\Gamma(xe^{-rt}, \bar{\tau} - t)\,d\bar{\tau} \\ -\Gamma(xe^{-rt}, \tau_{\max} - t)]e^{-(\gamma+r)t} & 0 \le t \le \tau_{\max} \\ 2\int_0^{\tau_{\max}} f(\bar{\tau})\mathcal{F}(u(t-\bar{\tau}, xe^{-r\bar{\tau}}))e^{(\gamma+r)\bar{\tau}}\,d\bar{\tau} \\ -\mathcal{F}(u(t-\tau_{\max}, xe^{-r\tau_{\max}}))e^{(\gamma+r)\tau_{\max}} & \tau_{\max} < t. \end{cases} \tag{9b}$$

Equations (9a) and (9b) are the fundamental result of this section and clearly demonstrate the time retardation $(t - \bar{\tau})$ as well as the spatial retardation $(xe^{-r\bar{\tau}})$ that makes this particular problem so interesting.

In the event that the distribution of ages at cytokinesis is sharply peaked so the density is approximated by a delta function, $f(\bar{\tau}) = \delta(\tau - \bar{\tau})$ with $\tau_{\max} = \tau > 0$, then this temporal and spatial retardation is even more clearly evident since (9a,b) become

(10)
$$\frac{\partial u}{\partial t} + rx\frac{\partial u}{\partial x} = -[\gamma + r]u + \begin{cases} \Gamma(xe^{-rt}, \tau - t)e^{-(\gamma+r)t} & 0 \le t \le \tau, \\ \mathcal{F}(u(t-\tau, xe^{-r\tau}))e^{(\gamma+r)\tau} & \tau < t. \end{cases}$$

In this paper we focus on the solution properties of equation (10).

Though the assumption that $f(\bar{\tau})$ can be approximated by a delta function may seem extreme, there are several reasons to make it. First, given the fact that nothing is known about the general solution properties of equations (9a) and (9b), it is reasonable to first explore the behavior of (10) obtained by assuming $f(\bar{\tau}) = \delta(\tau - \bar{\tau})$. Secondly, from the work of Anderson [1], we know that as long as the variance $\sigma_{\bar{\tau}}^2$ of $\bar{\tau}$ relative to its mean value squared $\langle\bar{\tau}\rangle^2$ remains small, the qualitative features of the solutions of (9a), (9b), and (10) should be the same. Finally, in a model [10] for the regulation of cellular numbers within the mammalian pluripotential stem cell population that is quite similar to the one developed here except that maturation is not included, it was found that: (1) The model *quantitatively* accounts for a wide variety of dynamic data in humans and dogs displaying periodic hematopoiesis or aplastic anemia; and (2) The model offers quantitative predictions concerning stability and instability of cellular populations that have been experimentally verified in mice [6, 7].

3. A particular example. In studying the behavior of equation (10), we take the function $\mathcal{F}$ to be given by

$$\mathcal{F}(u) = u(1 - u),$$

set

$$\delta = \gamma + r, \qquad \alpha = e^{-r\tau}, \quad \text{and} \quad \lambda = e^{(\gamma+r)\tau}$$

and take an initial function $u(t', x') = \varphi(x')$ for $0 \le t' \le \tau$ and $0 \le x' \le 1$ so (10) becomes

$$\frac{\partial u}{\partial t} + rx\frac{\partial u}{\partial x} = -\delta u + \lambda u(t-\tau, \alpha x)[1 - u(t-\tau, \alpha x)] \qquad \tau < t. \tag{11}$$

A number of authors [**8, 3, 4, 12, 13, 14, 9**] have studied the global stability properties of a class of partial differential equations that includes equation (11) when $\tau = 0$. These results indicate that when $\varphi(0) > 0$ the solutions of (11) (with $\tau = 0$) will be globally asymptotically stable. However, when $\varphi(0) = 0$ the solutions are chaotic on a function space in the sense that $\lim_{t\to\infty} u(t,x)$ is sensitively dependent on $\varphi(x)$. There are no analytic results to give insight into solution behavior when $\tau > 0$. In the remainder of this paper we study the solutions of (11) and variants of its to obtain insight into the modes of dynamic behavior that are possible, their dependence on the initial function φ, and how these are separately influenced by the time retardation and the spatial retardation.

4. Numerical methods. Equation (11), with the appropriate initial and boundary conditions, is solved using the Galerkin Finite Elements method [**5**]. Briefly, given a partial nonlinear differential equation $L(u) = 0$ in a domain D, with the appropriate initial and boundary conditions in D, the method assumes that u is accurately represented by an approximate solution u_a:

$$u_a(t,x) = \sum_{j=1}^{N} u_j(t)\phi_j(x) \tag{12}$$

where the ϕ_j's are the known basis functions and the u_j's are the unknown coefficients. N is the number of nodes in the spatial discretization. Since the basis functions are chosen to be equal to one at the nodes, the unknown coefficients u_j are equal to the approximate solution u_a at the nodes. Substitution of (12) into the equation $L(u) = 0$ gives the nonzero residual R:

$$R = L(u_a) = L\left(\sum_{j=1}^{N} u_j\phi_j\right). \tag{13}$$

To obtain the unknown coefficients, the residual R is forced to zero in the following integral sense:

$$F_k = (R, \phi_k) = \int_D R\phi_k \, dx \tag{14}$$

where the ϕ_k's are the weighting functions. In the Galerkin method these are equal to the basis functions. If L is a nonlinear differential operator, the spatial discretization leads to a set of nonlinear ordinary differential equations $F_k = 0$, $k = 1, \ldots, N$. The time derivatives can now be discretized and the resulting set of nonlinear equations is solved by using, for example, a Newton-Raphson scheme.

In this paper we use linear basis and weighting functions. The spatial domain consists of thirty elements ($N = 31$). A uniform node distribution is used except for the cases where a boundary layer develops. The time integration scheme is a first order predictor-corrector method (Forward Euler-Backward Euler) with a fixed time step $h = \tau/100$. The resulting implicit set of nonlinear algebraic equations for the unknown coefficients u_j are solved using the Newton-Raphson iteration scheme.

5. Numerical results. In discussing the solution properties of equation (11) and variants of it, we first consider the situation in which the initial function satisfies $\varphi(0) > 0$ in Case A, followed by $\varphi(0) = 0$ as Case B. Throughout, we fix the parameters $\delta = 1$, $\lambda = 2$, and when $\tau \neq 0$ we take $\tau = 1$.

Case A. $\varphi(0) > 0$.

In the event that $\tau = 0$, equation (11) is easily solved by the method of characteristics to give

$$u(t,x) = \frac{(\lambda - \delta)\varphi(xe^{-rt})e^{(\lambda-\delta)t}}{(\lambda - \delta) + \lambda\varphi(xe^{-rt})[e^{(\lambda-\delta)t} - 1]}. \tag{15}$$

It is clear from (15) that when $\varphi(0) > 0$ we have the long time limit of $u(t,x)$ approaching a spatially uniform steady state

$$u_{ss} = \lim_{t\to\infty} u(t,x) = \frac{\lambda - \delta}{\lambda} \tag{16}$$

that, by the results of [8], is globally asymptotically stable. For the parameter values we have chosen, this steady state is $u_{ss} = 1/2$.

This behavior is illustrated in Figure 1 where we show the numerically computed time (Figure 1a) and spatial (Figure 1b) behavior of the solution of (11) with $\tau = 0$ and an initial condition $\varphi(x) = 0.1 + x$.

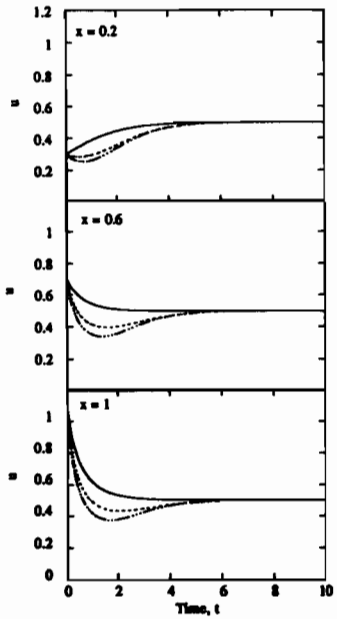

FIGURE 1a. Cell density behavior in the absence of any retardation with $\varphi(x) = 0.1 + x$. a. Top $x = 0.2$, middle $x = 0.6$, bottom $x = 1.0$. —— $\tau = 0.1$, – – – $\tau = 1.0$, – · · · – $\tau = 1.5$. Time t: —— 0, – – – 2, – · · · – 10.

(This is the same initial condition we use throughout this section.) The computed behavior is in strict accord with the analytic solution (15).

To investigate the effect of including the time retardation and neglecting the spatial retardation, in (11) we took $\alpha = 1$ and computed the numerical solutions of

$$\frac{\partial u}{\partial t} + rx\frac{\partial u}{\partial x} = -\delta u + \lambda u(t-\tau, x)[1 - u(t-\tau, x)], \qquad \tau < t. \tag{17}$$

In studying this case numerically, any solution vector $u_j(t', x_j)$ is stored for a time t and used in $u_{\tau j} = u_j(t-\tau, x_j)$ when $t' = t - \tau$.

As in the case when $\tau = 0$, we know that one steady state should be given by equation (16) since, in the long time limit, the time delay should play no role. However, in contrast to the case with $\tau = 0$, we do not know if these solutions are globally asymptotically stable. The

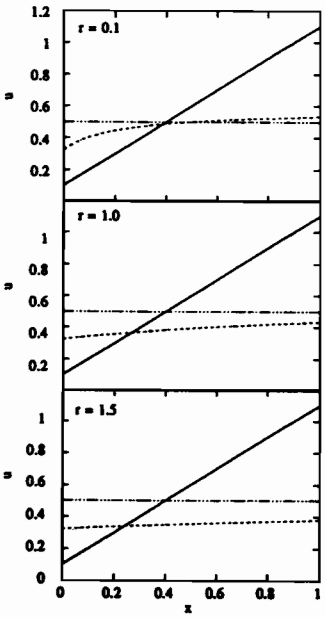

FIGURE 1b. Top $r = 0.1$, middle $r = 1.0$, bottom $r = 1.5$.

results shown in Figure 2a indicate that the homogeneous steady state of $u_{ss} = 1/2$ is stable since we found $u(t,x)$ evolving to $1/2$ for all values of x and the parameter r. However, the effect of the time delay is to slow the approach of $u(t,x)$ to the homogeneous solution relative to the case when $\tau = 0$ (compare with Figure 1b). Further, at early times ($t = 2$), it is found that the profiles exhibit a spatial maximum whose location increases with increasing r. This is in contrast to the situation without delay (Figure 1b) in which the profiles are always monotone.

We next considered the effect of the spatial retardation in the absence of the temporal delay by numerically solving the equation

$$\frac{\partial u}{\partial t} + rx\frac{\partial u}{\partial x} = -\delta u + \lambda u(t,\alpha x)[1 - u(t,\alpha x)]. \tag{18}$$

Numerically, the solution vector $u_j(t,x)$ is used to obtain $u_j(t, x_j e^{-rt})$ by a linear interpolation scheme. Since an iteration scheme is used to

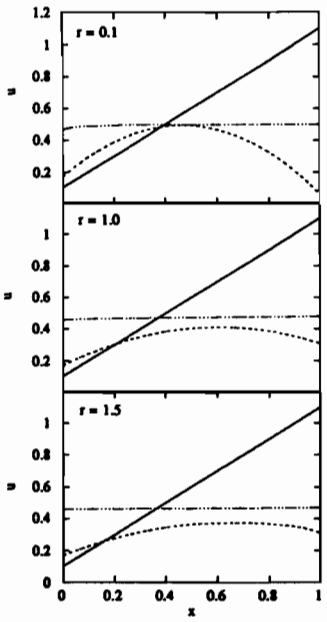

FIGURE 2a. Cell density profiles with $\varphi(x) = 0.1 + x$. Top $r = 0.1$, middle $r = 1.0$, bottom $r = 1.5$. Time t: —— 0, – – – 2, – · · · – 10. Temporal retardation only.

solve for the solution vector u_j, the linear interpolation is done for each Newton-Raphson iteration.

The effect of this nonlocal effect on the dynamics is illustrated in Figure 2b, in which it appears that once again the solutions are approaching a homogeneous steady state $u_{ss} = 1/2$. A comparison of these solutions with those shown in Figure 1b indicates that the nonlocal effects do not slow the approach of $u(t, x)$ to a homogeneous solution and, in fact, tend to make the spatial variation of u less than when the nonlocal effects are absent.

Finally, we numerically explored the behavior of the full equation (11) with the parameter values indicated above and $\varphi(x) = 0.1 + x$. To numerically solve the equation in this case, the two previous schemes used to shift the independent variables are used, but now the spatial shifting is done once at time t' and stored as $u_j(t', x_j e^{-r\tau})$ and used in $u_{\tau j} = u_j(t - \tau, x_j)$ when $t' = t - \tau$.

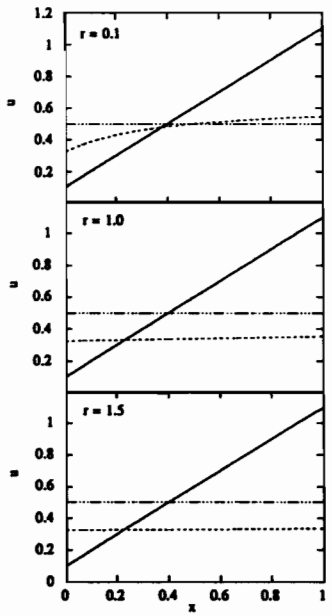

FIGURE 2b. Spatial retardation only.

From the previous results with either the temporal retardation or the spatial retardation, one would expect that the only stationary solution of equation (11) should be the homogeneous solution $u_{ss} = 1/2$. It is expected that the delay effect will slow the dynamics of approach to the stationary state. At early times the spatial dependence of the cell density will be affected by two competing effects: the time delay tends to produce profiles exhibiting a maximum while the nonlocal effects produce monotonically increasing profiles.

The cell density profiles are shown in Figure 2c. For any r, the solutions always appear to evolve toward the homogeneous state, $u_{ss} = 1/2$.

r = 0.1. Comparing Figures 2c and 1b shows that the solution approaches the homogeneous solution but at a slower rate due to the delay effect. Comparing Figures 2c and 2a shows that both solutions approach the homogeneous solution with the same time scales. At

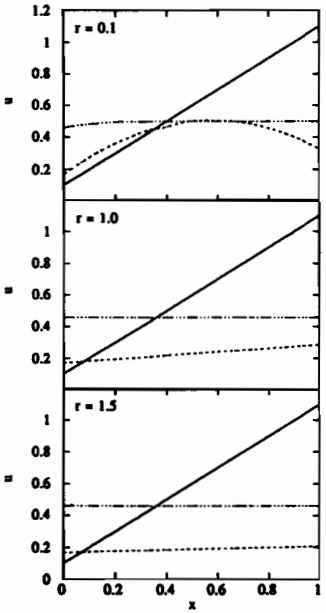

FIGURE 2c. Both.

$t = 2$, nonlocal effects tend to reduce the curvature by increasing $u(2, x = 1)$. Comparison of Figures 2c and 2b shows that the dynamics are slower and that the profile at early times ($t = 2$) exhibits a maximum due to the time delay effect.

r = 1. Comparison of Figures 2c and 1b shows the slower dynamics due to the time delay effect. Comparison of Figures 2c and 2a shows that the solutions approach $u_{ss} = 1/2$ with the same time scale since both solutions are retarded by the same delay. The nonlocal effects at early times ($t = 2$) produce a monotonically increasing cell density. Comparison of Figures 2c and 2b shows a slower dynamics due to the delay effect. At early times ($t = 2$) both profiles are monotonic due to nonlocal effects.

r = 1.5. Same trends as with $r = 1$.

Thus, in conclusion, it seems that when $\varphi(0) > 0$ there is a unique stationary solution to (11) given by equation (16). The net effect of

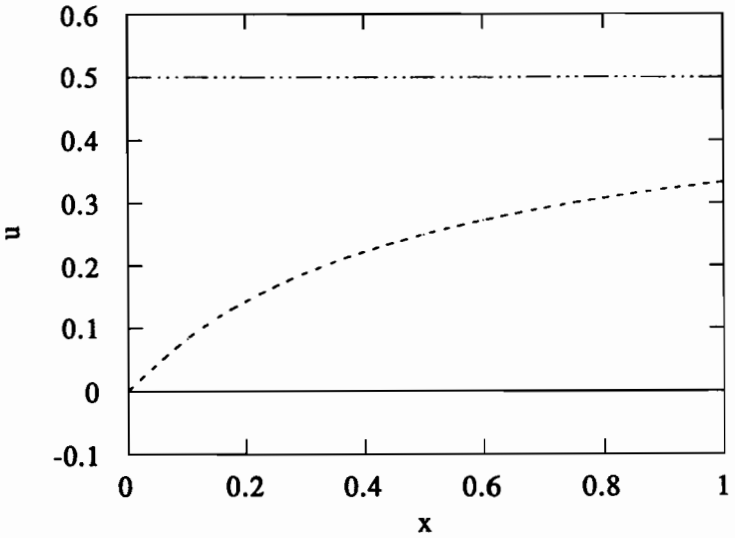

FIGURE 3. Stationary solutions without temporal or spatial retardation when $\varphi(x) = x$ as predicted by equation (19). —— $r > 1$, – – – $r = 1$, – · · · – $r < 1$.

the time delay is to retard the dynamics, while nonlocal effects tend to modify the cell density distribution. The strength of the two effects depends on position, time, and the magnitude of r.

Case B. $\varphi(0) = 0$ *Induces multistability and boundary layer formation.*

When $\varphi(0) = 0$, the case in which Lasota [8] has shown that the solutions of (11) with $\tau = 0$ are chaotic in a function space, the behaviors of (11) with $\tau > 0$ are quite interesting from several perspectives. In this section we present aspects of these as determined numerically with $\varphi(x) = x$ throughout.

First note that if $\tau = 0$ and $\varphi(x) = x$ then the analytic solution (15) no longer has a unique globally asymptotically stable uniform steady state given by (16). Rather, it is trivial to show that

$$u_{xx}(x) = \lim_{t\to\infty} u(t,x) = \begin{cases} 0 & 0 \le \lambda - \delta < r \\ \frac{(\lambda-\delta)x}{(\lambda-\delta)+\lambda x} & r = \lambda - \delta \\ \frac{\lambda-\delta}{\lambda} & r < \lambda - \delta, \end{cases} \tag{19}$$

thus illustrating the loss of stability of the solutions $u(t,x)$ when

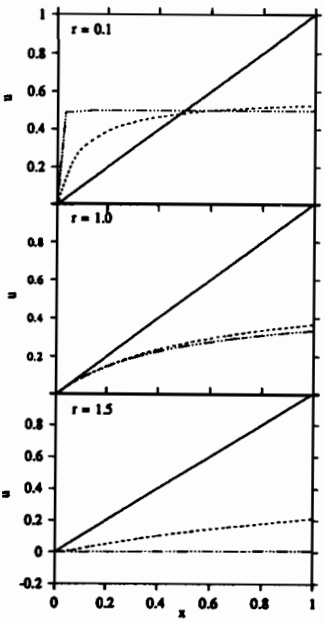

FIGURE 4. Spatial dependence of cell density profiles for $\varphi(x) = x$. Top $r = 0.1$, middle $r = 1.0$, bottom $r = 1.5$. Time t: —— 0, – – – 2, –·–·– 10.

$\varphi(0) = 0$. The steady state solutions of equation (19) are plotted in Figure 3 for the parameter values used here.

The cell density $u(t, x)$ profiles are shown in Figure 4. Depending on the value of r, numerically the solution evolves towards the steady states detailed in (19). In the case of $r = 1$, which is the critical value for the parameters we have chosen, the nonhomogeneous steady state is

$$u_{ss} = \frac{x}{1 + 2x}.$$

For $r = 0.1$ a boundary layer develops in the neighborhood of 0. Since there is no diffusive mechanism, the layer thickness decreases with increasing times and the solution is singular as $t \to \infty$. For $r = 1.5$, the profiles remain linear and the cell density tends to an extinguished ($u_{ss} = 0$) state at large times.

The boundary layer behavior is present whenever $r < 1$, and the

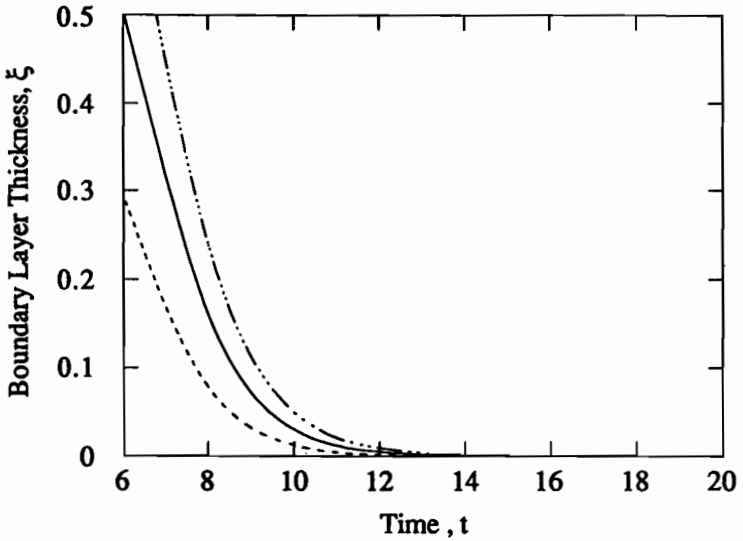

FIGURE 5. Dynamics of boundary layer thickness defined by equation 20. —— $r = 0.01$, – – – $r = 0.1$, –·····– $r = 0.15$.

solution evolves to the homogeneous profile $u_{ss} = 1/2$ for $x > 0$. The boundary layer thickness ξ is defined as:

$$\varepsilon = \frac{1}{2} - u(t,\xi) = \frac{\xi e^{(\lambda-\delta-r)t}}{1 + \lambda\xi[e^{(\lambda-\delta-r)t} - e^{-rt}]} \tag{20}$$

where $\varepsilon \ll 1$. In what follows, we take $\varepsilon = 10^{-3}$. The dynamics of the boundary layer is illustrated in Figure 5. At any given time ξ decreases with increasing r. The figure demonstrates the singular behavior of the solutions since $\lim_{t\to\infty} \xi = 0$.

Drawing an analogy between bifurcations and phase transition, the nonuniform cell density that exists for $r = 1$ [cf. Equation (19)] can be thought of as representing a critical point separating the two spatially homogeneous solutions $u_{ss} = 1/2$ for $r < 1$ and $u_{ss} = 0$ for $r > 1$. Extending this further, one would expect that the phenomenon of critical slowing down should be present for $1 - \varepsilon < r < 1 + \varepsilon$. This expectation is borne out in the plots of Figure 6 where we show the cell density $u(t,x)$ as a function of time at different locations. For $r = 1$, the solution quickly converges to the nonuniform steady state $u_{ss} = x/(1 + 2x)$ of equation (19), but for the other two cases the solutions first evolve to the corresponding nonhomogeneous steady

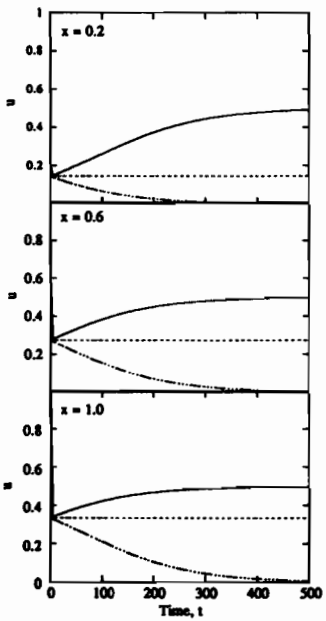

FIGURE 6. Critical slowing down of cell density dynamics in the absence of temporal and spatial retardation when $\varphi(x) = x$. Top $x = 0.2$, middle $x = 0.6$, bottom $x = 1.0$. —— $r = 0.99$, – – – $r = 1.0$, – · · · – $r = 1.01$.

states and later slowly diverge towards their corresponding steady states.

We next examined the effect of having only a temporal retardation with an initial condition $\varphi(x) = x$ by numerically studying equation (17). The results are summarized in Figure 7a where the same r values as in Figure 4 are used. The steady state solutions of equation (17) are once again given by equation (19) since the time delay will have no effect on the long time behavior, and are thus those of Figure 3. For $r = 0.1$, the effect of the time delay is to slow the evolution towards the singular steady state $u_{ss} = 1/2$, with an initially strong effect in the neighborhood of $x = 1$. For $r = 1$, there is once again a slower approach to the nonhomogeneous profile $u_{ss} = x/(1+2x)$. For $r = 1.5$, the time delay slows the approach to the extinguished solution $u_{ss} = 0$.

The effect of the spatial delay alone was examined by solving equa-

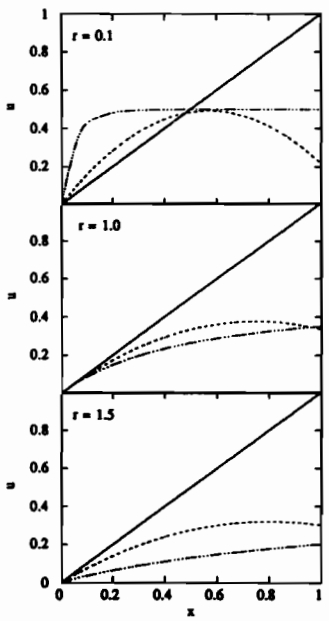

FIGURE 7a. Cell density profiles for $\varphi(x) = x$. Top $r = 0.1$, middle $r = 1.0$, bottom $r = 1.5$. Time t: —— 0, – – – 2, – · · · – 10. Temporal retardation only.

tion (18), and the results are shown in Figure 7b for the same values of the parameter r as before. In addition to different times of approach to the corresponding steady states, the solution evolves towards the extinguished solution $u_{ss} = 0$ for $r = 1$ instead of the nonhomogeneous state. For $r = 0.1$, the cell density approaches the singular solution $u_{ss} = 1/2$. For $r = 1.5$, the solution rapidly approaches the extinguished state $u_{ss} = 0$.

A numerical parametric study of equation (18) shows that a nonhomogeneous stationary cell density does exist at a critical r given by $r_c = 0.234655$. This shift in r_c from 1 is due to the presence of nonlocal effects. Increasing τ in the spatial retardation factor $e^{-r\tau}$ will cause the critical value of r to decrease. Recalling that, in general, the closer r is to its critical value r_c, the slower the approach to the equilibrium, we expect that the shifting of r_c from 1 to $r_c = 0.234655$ will slow the dynamic approach of $u(t, x)$ to u_{ss} for $r = 0.1$ but hasten the approach

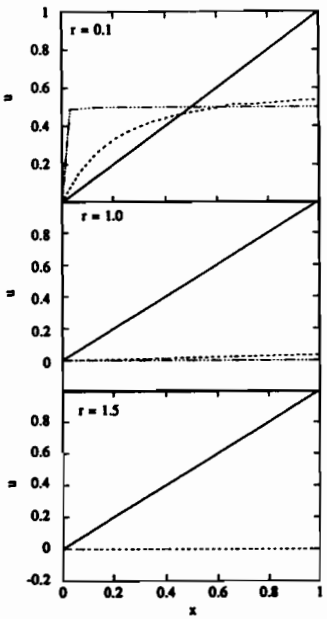

FIGURE 7b. Spatial retardation only.

for $r = 1$ and 1.5. This effect is quite obvious in comparing Figures 7b and 4.

Nonlocal effects not only shift the critical value of r_c but also the stationary nonhomogeneous cell density itself. The three steady state solutions to equation (18) are shown in Figure 8. For $r < 0.234655$, the stationary state is the singular solution $u_{ss} = 1/2$ for $x > 0$. For $r = 0.234655$, the stationary state monotonically increases from 0 to 0.432 and is larger than the $u_{ss} = x/(1 + 2x)$ found in the absence of the spatial retardation. For $r > 0.234655$, the stationary state is the extinguished state $u_{ss} = 0$.

Based on the results presented to this point, we would expect that the inclusion of both temporal and spatial retardation in equation (11) will result in different dynamics of approach to stationary states, in the presence of a different nonhomogeneous steady state, and in a shifting of the critical value r_c. The critical value of r should coincide with

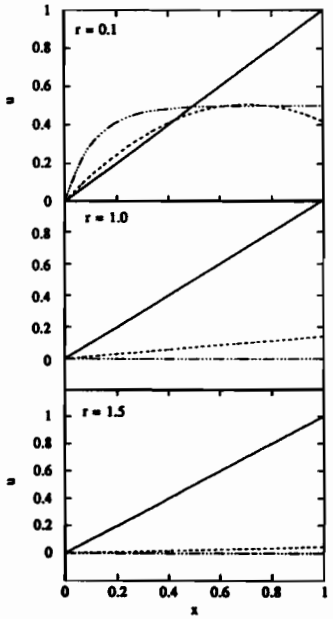

FIGURE 7c. Both.

that obtained for equation (18). Also, the presence of a critical slowing down in the proximity of the cross over region from the extinguished to the singular should be present.

Figure 7c shows the computed behavior of the cell density profiles $u(t, x)$. We discuss the solution behavior as a function of r.

r = 0.1. Comparing Figures 4 and 7c, we note that the solution again approaches the singular solution but at a slower rate due to the delay effect and also due to the fact that $r = 0.1$ is closer to its critical value. Comparing Figures 7a and 7c shows that the solutions with time delay only approach the singular solution somewhat faster since nonlocal effects slow down the dynamics due to the shifting of r_c. Comparison of Figures 7b and 7c shows that the dynamics are slower due to the time delay effect.

r = 1. Comparing Figures 4 and 7c shows that the solution approaches the extinguished solution due to the shifting of the critical

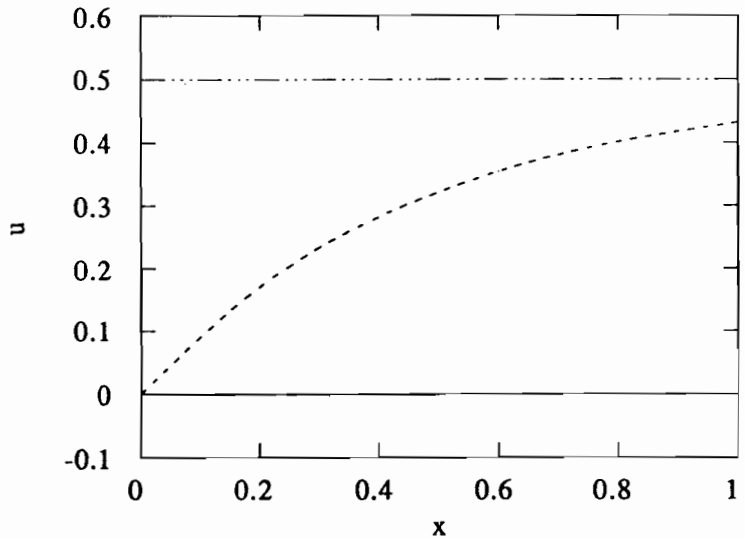

FIGURE 8. Stationary solutions of equation (11) with $\varphi(x) = x$. —— $r > 0.234655$, – – – $r = 0.234655$, – · · · – $r < 0.234655$.

parameter r_c. Comparing Figures 7b and 7c illustrates that the dynamics are slower due to the time delay effect.

r = 1.5. The results are qualitatively identical with those of $r = 1$.

As before, the three steady state solutions of equation (11) are those of equation (18) as illustrated in Figure 8.

The critical slowing down in the proximity of $r_c = 0.234655$ is shown in Figure 9 where the cell density is plotted for $x = 0.2$, 0.6 and 1 with $r = 0.23$, 0.234655, and 0.24. For $r < r_c$, the solutions slowly evolve towards the singular solution, for $r = r_c$ the solutions quickly converge to the nonhomogeneous steady state, and for $r > r_c$, the cell density slowly evolves towards the extinguished solution.

6. Summary. Here we have shown that a mathematical model for cell population dynamics, in which there is simultaneous proliferation and maturation, naturally results in a nonlinear first order partial differential equation in which there is retardation in both temporal and maturation variables. Numerical analysis of a representative equation indicates that there are two classes of solution behavior depending on the initial function $\varphi(x)$ of the population maturation variable x. If

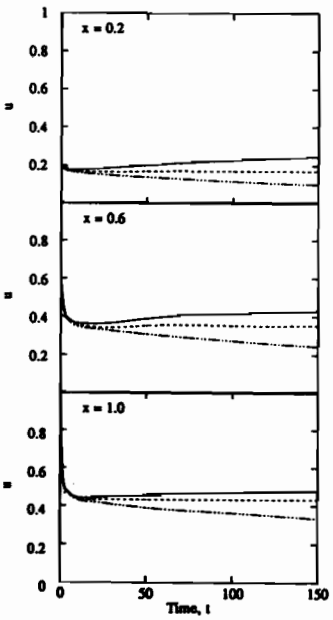

FIGURE 9. Critical slowing down of cell density dynamics with both spatial and temporal retardation and $\varphi(x) = x$. Top $x = 0.2$, middle $x = 0.6$, bottom $x = 1.0$. —— $r = 0.23$, − − − $r = 0.234655$, − · · · − $r = 0.24$.

$\varphi(0) > 0$ there is a unique stationary solution. In this case the net effect of the time delay is to retard the dynamic approach to the stationary solution, while spatial delays modify the steady state distributions with respect to the maturation variable. Alternately, if $\varphi(0) = 0$ the stationary solutions display a multistability that depends on the maturation velocity r. For a critical value $r = r_c$, which depends on the time delay, the stationary solution is nonhomogeneous. For values of r close to r_c, the solution dynamics exhibit critical slowing down, similar to that seen in the neighborhood of a phase transition. For $0 < r_c < r$, the stationary solution is uniformly zero, while for $0 < r < r_c$, the stationary solution is homogeneous and singular.

Acknowledgments. We thank the McGill University Computing Center for a grant to defray the computational costs of this research,

and the Natural Sciences and Engineering Research Council for operating grant support to both ADR and MCM. MCM also thanks NATO for a Collaborative Research Grant.

REFERENCES

1. R.F.V. Anderson, *Geometric and probabilistic stability criteria for delay systems*, Math. Biosci. **105** (1991), 81–96.

2. R. Baserga, *The biology of cell replication*, Harvard University Press, Cambridge, 1985.

3. P. Brunovský, *Notes on chaos in the cell population partial differential equation*, Nonlinear Anal. **7** (1983), 167–176.

4. P. Brunovský and J. Komorník, *Ergodicity and exactness of the shift on $C[0,\infty]$ and the semiflow of a first order partial differential equation*, J. Math. Anal. Appl. **104** (1984), 235–245.

5. C.A.J. Fletcher, *Computational Galerkin methods*, Springer-Verlag, New York, 1984.

6. C.M. Gibson, C.W. Gurney, E.O. Gaston and E.L. Simmons, *Cyclic erythropoiesis in the $S1/S1^d$ mouse*, Exper. Hemat. **12** (1984), 343–348.

7. C.W. Gurney, E.L. Simmons and E.O. Gaston, *Cyclic erythropoiesis in W/W^V mice following a single small does of ^{89}Sr*, Exper. Hemat. **9** (1981), 118–122.

8. A. Lasota, *Stable and chaotic solutions of a first order partial differential equation*, Nonlinear Anal. **5** (1981), 1181–1193.

9. K. Loskot, *Turbulent solutions of a first order partial differential equation*, J. Differential Equations **58** (1985), 1–14.

10. M.C. Mackey, *Unified hypothesis for the origin of aplastic anemia and periodic hematopoiesis*, Blood **51** (1978), 941–956.

11. M.C. Mackey and J.G. Milton, *Feedback, delays and the origin of blood cell dynamics*, Comm. Theor. Biol. **1** (1990), 299–327.

12. R. Rudnicki, *Invariant measures for the flow of a first order partial differential equation*, Ergodic Theory Dynamical Systems **5** (1985), 437–443.

13. ———, *An abstract Wiener measure invariant under a partial differential equation*, Bull. Polish Acad. Sci. Math. **35** (1987), 289–295.

14. ———, *Strong ergodic properties of a first order partial differential equation*, J. Math. Anal. Appl. **132** (1988), 14–26.

DEPARTMENT OF CHEMICAL ENGINEERING, MCGILL UNIVERSITY, 3480 UNIVERSITY STREET, MONTREAL, QUEBEC, CANADA H3A2A7

DEPARTMENTS OF PHYSIOLOGY AND PHYSICS AND CENTRE FOR NONLINEAR DYNAMICS IN PHYSIOLOGY AND MEDICINE, MCGILL UNIVERSITY, 3655 DRUMMOND STREET, MONTREAL CANADA H3G1Y6